Organic Electronics 13 (2012) 1392–1400

Contents lists available at SciVerse ScienceDirect

Organic Electronics

journal homepage: www.elsevier.com/locate/orgel

TIPS-triphenodioxazine versus TIPS-pentacene: Enhanced electron mobility for n-type organic field-effect transistors

Yohann Nicolas [a,*], Frédéric Castet [a], Mélanie Devynck [b], Pascal Tardy [b], Lionel Hirsch [b], Christine Labrugère [c], Hassan Allouchi [d], Thierry Toupance [a,*]

[a] University of Bordeaux, Institut des Sciences Moléculaires, UMR 5255 CNRS, 33405 Talence Cedex, France
[b] University of Bordeaux, Laboratoire de l'Intégration du Matériau au Système, UMR 5218 CNRS, ENSCBP, 16 Avenue Pey-Berland, 33607 Pessac Cedex, France
[c] CeCaMA, Centre de Caractérisation des Matériaux Avancés, Institut de Chimie de la Matière Condensée de Bordeaux, UPR 9048 CNRS, 87 Avenue du Docteur A. Schweitzer, F33608 Pessac Cedex, France
[d] Laboratoire de Chimie Physique PCBM, EA 4244, Faculté de pharmacie, 31 Avenue Monge, 37200 Tours, France

ARTICLE INFO

Article history:
Received 26 July 2011
Received in revised form 4 April 2012
Accepted 6 April 2012
Available online 21 April 2012

Keywords:
TIPS-pentacene
Triphenodioxazine
N-type
OFET

ABSTRACT

A new soluble n-type material based on the 2,9-bis(triisopropylsilylethynyl)triphenodioxazine (TIPS-triphenodioxazine) has been designed as a quinonoid equivalent of TIPS-pentacene and synthesized using an innovative synthetic pathway. Both materials showed identical electronic affinities, intermolecular arrangements and thin film topographies. However, the TIPS-triphenodioxazine led to better performances than TIPS-pentacene in n-channel organic field-effect transistors (OFETs) evidencing the potentialities of this π-conjugated core in the field of organic electronics.

1. Introduction

Over the past decade, organic electronics have attracted growing interest due to the potential and demonstrated advantages of organic materials compared to conventional inorganic analogs such as light weight, low-cost production, flexibility and large area coverage [1–3]. One of the main issues in this field is to elaborate organic electronic circuits, which require complementary p-channel and n-channel organic field-effect transistors combined with complementary metal-oxide semiconductor layouts in order to reduce the power consumption [4–6]. Although numerous works thoroughly report on the performances of p-type semi-conducting materials, the instability of n-channel OFET has delayed their integration in OFET architectures [7–10]. Thus, electron-withdrawing groups such as carbonyls [11] and halogenated functions [12–14] have been often added to the π-structure to reduce the LUMO energy level and stabilize the negative charges [15,16]. Despite recent results [17,18], the design of soluble n-type materials still remains an important challenge in organic electronics [19–23].

On the other hand, the TIPS-pentacene architecture has been described as a soluble and efficient p-type organic semiconductor [24]. TIPS-pentacene combines the pentacene core that ensures charge delocalization, and triisopropylsilylethynyl (TIPS) groups on the central ring, which confers solubility to it. Both components lead to a 2-D brick-layer arrangement of π-stacking [25] and mobility higher than 1 $cm^2 V^{-1} s^{-1}$ for solution-processable transistors [26]. In order to design soluble n-type materials, a recent strategy has consisted in lowering the LUMO energy level by the replacement of carbon and hydrogen atoms of TIPS-pentacene by nitrogen atoms [27,28]. The concept hereafter described, is also based on the stabilization of the anionic form, by substituting the pentacene core by

* Corresponding authors. Tel.: +33 5 40002425; fax: +33 5 40006994.
E-mail addresses: y.nicolas@ism.u-bordeaux1.fr (Y. Nicolas), t.toupance@ism.u-bordeaux1.fr (T. Toupance).

1566-1199/$ - see front matter © 2012 Elsevier B.V. All rights reserved.
http://dx.doi.org/10.1016/j.orgel.2012.04.010

the triphenodioxazine core. Indeed, unlike the aromatic core of pentacene, triphenodioxazines exhibit a quinonoid structure at the center of the pentacycle that is expected to enhance the stability of the anion. Thus, insoluble triphenodioxazines substituted by trifluoromethyl groups have shown good air-stability [29]. As a consequence, we report on the synthesis of a new soluble triphenodioxazine bearing TIPS groups and the characterization of its structure and electronic properties in solution and thin film. To ensure minimal changes in the supramolecular organization when replacing the pentacene by the triphenodioxazine core, the TIPS bulky groups were maintained in the center of the molecule. Then, the semiconducting properties of TIPS-triphenodioxazine were studied by using an OFET architecture and its transport properties were compared to those of TIPS-pentacene. Triphenodioxazine core appeared to be a promising material for n-channel OFET.

2. Experimental section

2.1. Synthesis

Diethyl ether and THF were distilled from sodium benzophenone ketyl prior to use. Other chemical reagents were purchased from Sigma–Aldrich, Alfa Aesar or TCI Europe and were used as received without further purification.

2.1.1. Synthesis of 3,6-bis(2-nitrophenoxy)-2,5-dibromo-2,5-cyclohexadiene-1,4-dione (**1**)

Under a N_2 atmosphere, potassium *tert*-butoxide (3.67 g, 32.7 mmol) was added to a solution of 2-nitrophenol (4.55 g, 32.7 mmol) in THF (100 mL) leading to the formation of a red solid. After stirring for 1 h, the mixture was poured into 400 mL of diethyl ether. Then, the precipitate was filtered under a N_2 atmosphere, rinsed with pentane and dried in vacuum oven to yield potassium 2-nitrophenoxide (5.66 g, 31.9 mmol). A 100 mL 2-necked round-bottom flask containing a stir bar was then charged with bromanil (6.25 g, 14.8 mmol) and dry dimethylacetamide (40 mL) under a N_2 atmosphere. Potassium 2-nitrophenoxide (5.16 g, 29.1 mmol) was added at room temperature. After stirring for 2 h, the mixture was poured into 1 N HCl solution (500 mL). The yellow precipitate was filtered and rinsed successively by water, 2% $NaHCO_3$ solution, water and diethylether. After drying in vacuum oven, compound **2** (7.31 g, 13.5 mmol, yield = 93%) was isolated as a yellow solid. ^{1}H NMR (300 MHz, $(CD_3)_2CO$) δ: 7.44 (m, 4H), 7.69 (td, 2H), 8.15 (dd, 2H). ^{13}C NMR (300 MHz, $(CD_3)_2CO$) δ: 173.6, 153.6, 149.6, 135.6, 126.9, 125.75, 125.67, 119.7, 116.1. MS (ESI-TOF) calculated for $C_{18}H_8Br_2N_2O_8$ $[M^-]$: 537.9, found 537.9. Elemental microanalysis: $C_{18}H_8Br_2N_2O_8$ (540.07) calculated: C 40.0, H 1.5, N 5.2; found: C 39.0, H 1.5, N 5.0.

2.1.2. Synthesis of 2,9-dibromotriphenodioxazine (**2**)

In a 2-necked round-bottom flask containing a stir bar, compound **1** (1.34 g, 2.48 mmol), Fe (4.5 g, 80.7 mmol) and THF (50 mL) were heated at reflux. Acetic acid (12 mL, 210 mmol) was then added dropwise during 1 h and the mixture was stirred for a further 2 h. After filtration to remove the excess of iron, chloranil (4.5 g, 18.3 mmol) was added to the colorless solution. After stirring for 1 night, the red precipitate was filtered, rinsed successively with acetone, water, 2% $NaHCO_3$ solution, water, acetone and finally dried in vacuum oven 2 h. Compound **2** (956 mg, 2.15 mmol, yield = 87%) was obtained as a red solid. ^{1}H NMR (200 MHz, $C_2D_2Cl_4$, 130 °C) δ: 7,73 (d, 2H) ; 7,8 (m, 6H). The solubility of **2** was too low in common organic solvent to record suitable ^{13}C NMR data. MS (MALDI-TOF) calculated for $C_{18}H_8Br_2N_2O_2$ $[M^+]$: 441.9, found 441.9. Elemental microanalysis: $C_{18}H_8Br_2N_2O_2$ (444.08) calculated: C 48.7, H 1.8, N 6.3; found: C 47.2, H 2.0, N 6.0.

2.1.3. Synthesis of 2,9-bis(triisopropylsilylethynyl)triphenodioxazine (**3**) (TIPS-triphenodioxazine)

Under a N_2 atmosphere, tetrakis(triphenylphosphine)palladium (30 mg, 0.026 mmol), 2-(dicyclohexylphosphino)biphenyl (20 mg, 0.057 mmol), tetrabutylammonium acetate (330 mg, 1.10 mmol), (triisopropylsilyl)acetylene (195 mg, 1.07 mmol), compound **2** (200 mg, 0.450 mmol) and dimethylformamide (25 mL) were introduced in a Schlenk tube containing a stir bar. After stirring for 24 h at 90 °C, the mixture was poured into a solution of 1 N HCl (200 mL) and the product was extracted into dichloromethane. After drying over $MgSO_4$ and evaporation of the volatiles, the crude product was purified by column chromatography over silica gel (cyclohexane/toluene: 50/50) then by recrystallization in cyclohexane to give compound **3** (130 mg, 0.201 mmol) as a red solid in a 45% yield. ^{1}H NMR (250 MHz, CD_2Cl_2) δ: 1.22 (s, 42H), 7.13 (dd, 2H), 7.22 (td, 2H), 7.31 (td, 2H), 7.52 (dd, 2H). ^{13}C NMR (400 MHz, CD_2Cl_2) δ: 149.7, 149.6, 144.2, 135.3, 129.8, 128.8, 125.5, 115.4, 104.7, 101.4, 96.5, 18.5, 11.4. ESI-TOF HRMS: calculated for $[MH]^+$ ($C_{40}H_{51}N_2O_2Si_2$): 647.3483, found: 647.3477, δ = 1.02 ppm. Elemental microanalysis: $C_{40}H_{50}N_2O_2Si_2$ (647.01) calculated: C 74.2, H 7.8, N 4.3; found: C 73.8, H 7.7, N 4.2.

2.2. Instrumentation and methods

^{1}H and ^{13}C{^{1}H} NMR spectra were recorded on a DPX-300 spectrometer (δ given in ppm relative to tetramethylsilane). Electrospray mass spectra (ESI-TOF HRMASS) were carried out on a Qstar Elite mass spectrometer (Applied Biosystems). The electrospray needle was operated at room temperature. Spectra were recorded in the positive-ion mode using the reflextron and with an accelerating voltage of 20 kV (high resolution). MALDI-MS spectra were carried out on a Voyager mass spectrometer (Applied Biosystems) equipped with a pulse N2 laser (337 nm) and a time-delayed extracted ion source. Spectra were recorded in the positive-ion mode using the reflextron and with an accelerating voltage of 20 kV.

Cyclic voltammetry studies were carried out with a potentiostat/galvanostat Autolab PGSTAT100 using a three-electrode device (working electrode: Pt disc; reference electrode: Ag/AgCl calibrated with ferrocenium/ferrocene as internal reference; counter-electrode: Pt). UV–Vis

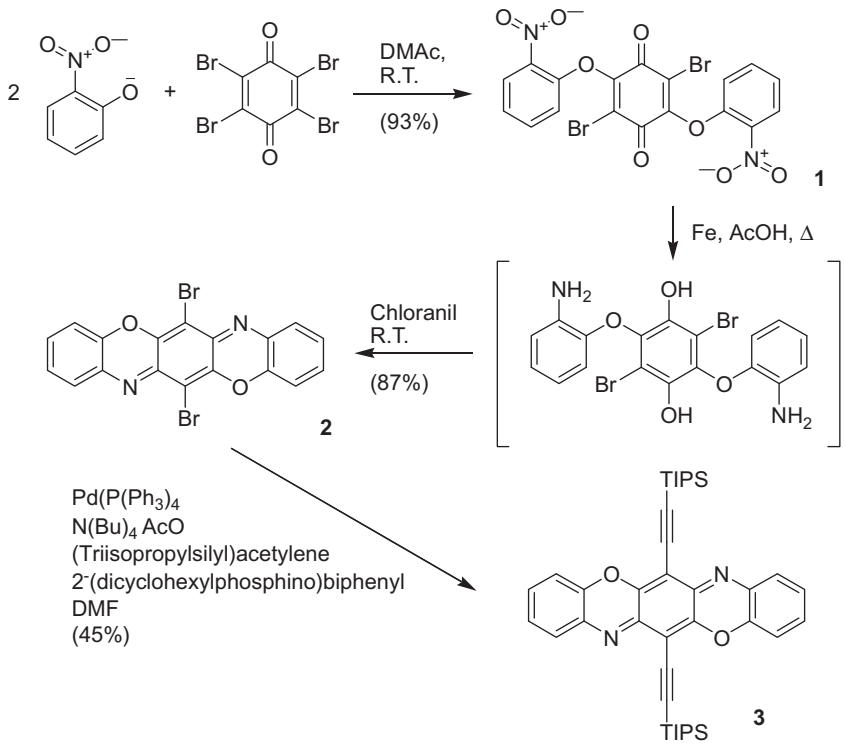

Scheme 1. Synthetic route towards TIPS-triphenodioxazine.

absorption studies have been carried out with a UV-1650PC SHIMADZU spectrophotometer. The spectra of TIPS-pentacene and TIPS-triphenodioxazine have been recorded in CH_2Cl_2 or as thin films deposited by sublimation on a spin-coated polystyrene thin film on glass substrates. Ultraviolet photoelectron spectroscopy (UPS) spectra of TIPS-pentacene and TIPS-triphenodioxazine have been performed on thin films sublimated on 100 nm thin film of gold deposited on glass substrates. The UPS spectra were collected with constant 3 eV pass energy at room temperature by a VG Scientific 220 i-XL ESCALAB spectrometer with UV lamp (He $I = 21.22$ eV) activated by a helium partial pressure of 10^{-5} Pa. The spot size was about 150 μm in diameter.

Atomic force microscopy (AFM) images of the material surface have been recorded on the channel of devices by a VEECO 3100 Digital Instrument used in tapping mode with a AC160TS Olympus tetrahedral cantilever. Single crystals of TIPS-triphenodioxazine were grown by slow evaporation of a saturated CH_2Cl_2 solution. A single crystal was mounted on an Xcalibur equipped with a monochromatized Mo-Kα source (0.71073 Å). Data collection, unit cell refinement, and data reduction were performed using the CrysAlis, Oxford Diffraction Ltd. software package. The positions of non-H atoms were determined and refined by SHELX-97 program. The positions of H atoms were deduced from coordinates of the non-H atoms and Fourier synthesis. H atoms were included for structure factor calculations but not refined. X-ray diffraction (XRD) studies were carried out with a Bruker AXS diffractometer (D2 PHASER A26-X1-A2B0D3A) using a Cu anode (Cu Kα radiation, $\lambda = 1.5405$ Å). The diffractograms were directly recorded from OFETs and samples without organic semiconducting materials and/or gold layers. The OFET substrates recovered with sublimated gold layer were used as reference to correct 2θ values in function of the sample height.

2.3. Theoretical calculations

All calculations were performed using the GAUSSIAN 09 package [30].

3. Results and discussion

3.1. Synthesis of TIPS-triphenodioxazine

The synthesis of the 2,9-bis(triisopropylsilylethynyl)triphenodioxazine **3** was achieved in three steps with an overall yield of 35 % (Scheme 1). As conventional routes usually involve strong oxidizing procedures limiting the variety of substituents that can be introduced on the triphenodioxazine core [31], a new synthetic pathway has been developed to obtain the dibromotriphenodioxazine **2** intermediate using mild conditions. First of all, a double addition of potassium 2-nitrophenoxide on tetrabromo-1,4-benzoquinone yielded the 3,6-bis(2-nitrophenoxy)-2,5-dibromoparabenzoquinone **1**. Then, the nitro group and benzoquinone moiety were reduced into amino and phenol functions by iron in acetic acid. The resulting unstable intermediate was then partially oxidized by chloranil to give a quinone derivative which immediately underwent a

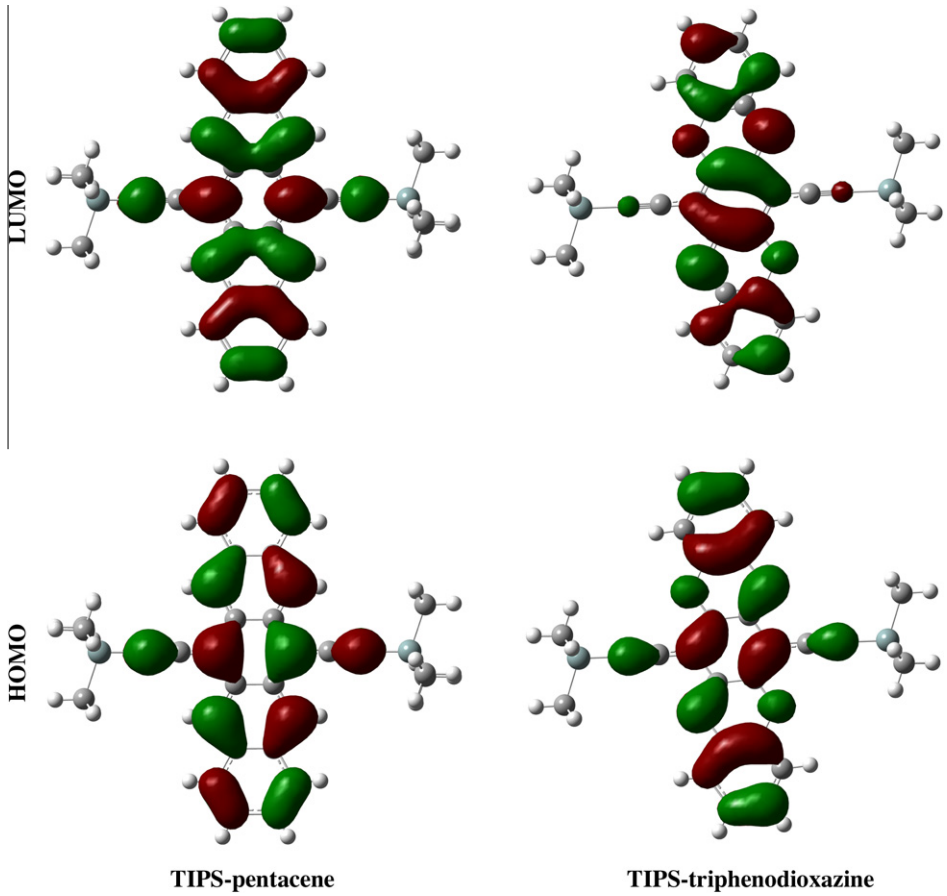

Fig. 1. Spatial distribution of frontier molecular orbitals, HOMO (top left) and LUMO (bottom left) of TIPS-pentacene, HOMO (top right) and LUMO (bottom right) of TIPS-triphenodioxazine.

Table 1
Electronic properties of TIPS-pentacene and TIPS-triphenodioxazine.

Compd.	Solution				Thin film		
	HOMO (eV)[a]	LUMO (eV)[a]	$E_{1/2,\ ox.}$ (V)[b]	$E_{1/2,\ red.}$ (V)[b]	E_{gap} (eV)[c]	I.E. (eV)[d]	E.A. (eV)[e]
TIPS-pentacene	−5.02	−3.14	0.35	−1.52 (−1.5[g])	1.63	5.92 (5.84[h])	4.29
TIPS-triphenodioxazine	−5.50	−3.14	0.74	−1.45	2.02	6.29	4.27
Δ[f]	−0.48	0	0.39	0.07		0.37	−0.02

[a] B3LYP/6-31G+(d,p) calculations using the IEF-PCM solvation model with CH_2Cl_2 as solvent.
[b] First oxidation and reduction potentials (vs ferrocenium/ferrocene Fc^+/Fc) measured by cyclic voltammetry in CH_2Cl_2 containing 0.1 M $TBAPF_6$ as salt support.
[c] Optical bandgap determined at the edge of the absorption band by UV–Vis absorption spectroscopy of a thin film deposited on a polystyrene/glass substrate.
[d] Ionization energy versus vacuum energy measured by UPS of a 7 nm-thick thin film deposited on gold surface.
[e] Electronic affinity calculated as the difference between I.E. and E_{gap}.
[f] Difference between electronic properties of TIPS-triphenodioxazine and TIPS-pentacene.
[g] Litt. [34].
[h] Litt. [35].

condensation and cyclization with the amino groups. Finally, the silylethynyl groups were introduced by a Sonogashira coupling under Cassar conditions [32,33]. As expected, TIPS-triphenodioxazine was soluble in most organic solvents and could also be sublimated under high vacuum.

3.2. Electronic properties

The structures of TIPS-triphenodioxazine and TIPS-pentacene were optimized using the density functional theory (DFT) at the B3LYP/6-31G* level. The wavefunctions

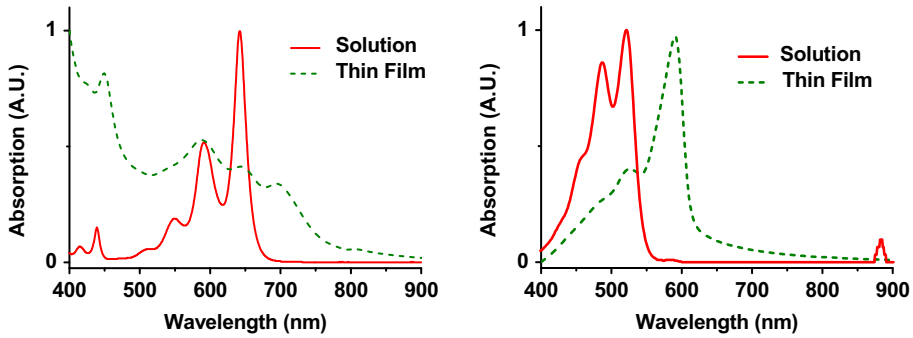

Fig. 2. UV–Vis absorption spectra of TIPS-pentacene (left) and TIPS-triphenodioxazine (right) in CH_2Cl_2 (red curve) and as thin films (green curve) (For interpretation of the references to color in this figure legend, the reader is referred to the web version of this article).

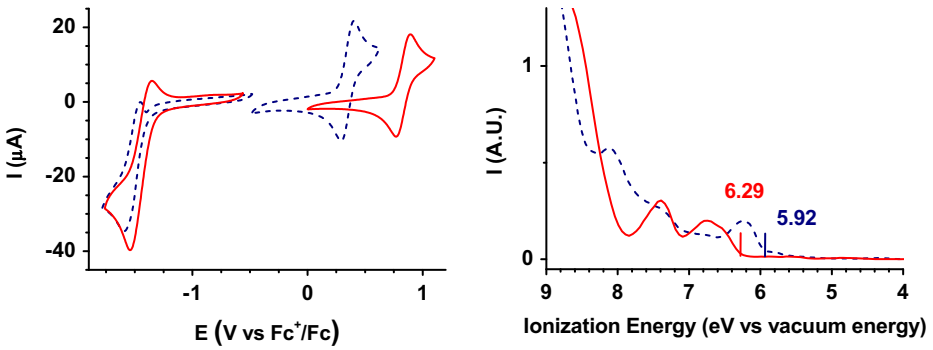

Fig. 3. Cyclic voltammogram (left) of TIPS-pentacene (in blue) and TIPS-triphenodioxazine (in red), UPS (right): first ionization bands of TIPS-pentacene (in blue) and TIPS-triphenodioxazine (in red) thin films sublimed on gold (For interpretation of the references to color in this figure legend, the reader is referred to the web version of this article).

were further refined at the B3LYP/6-31G+(d,p) level using the polarizable continuum model in its integral equation formalism (IEF-PCM) to account for solvent (dichloromethane) effects. The spatial distributions of the HOMO and LUMO, depicted in Fig. 1, clearly underline the aromatic character of TIPS-pentacene versus the quinonoid nature of TIPS-triphenodioxazine. Strikingly, when going from TIPS-pentacene to TIPS-triphenodioxazine, the HOMO shifts by 0.48 eV toward lower energies, while the LUMO energies are similar (Table 1).

To get a deeper insight into the electronic properties of the TIPS-triphenodioxazine both in solution and in the solid state, the optical band-gaps were inferred from UV–Vis spectra (Fig. 2), the reduction and oxidation potentials have been measured by cyclic voltammetry in CH_2Cl_2, and the ionization energies have been determined by ultra-violet photoelectron spectroscopy (UPS) (Fig. 3, see also Supplementary data).

The electron affinities have been calculated as the difference between the ionization energies and the UV–Vis absorption band edge of thin films. The corresponding data are gathered in Table 1. Whatever the experimental approach used to estimate the energy levels, the difference between the HOMO energy levels of TIPS-pentacene and TIPS-triphenodioxazine was found to be about 0.4 eV whereas their LUMO energy levels were similar, in very close agreement with DFT calculations. Furthermore, the cyclic voltammogram of TIPS-triphenodioxazine revealed a higher reversibility of the first reduction step evidencing a higher stability of the radical anion. At last, the absorption edges underwent a red-shift of 0.25 eV between the solution and the thin film spectra for both molecules, which suggests the existence of intermolecular interactions with comparable magnitudes for both compounds.

3.3. Crystal structure and supramolecular organization

Comparative multi-scale studies of solid state materials have been performed by single-crystal X-ray crystallography, powder X-ray crystallography and Atomic Force Microscopy (AFM) on thin films. At first, the crystallographic data of TIPS-triphenodioxazine showed a packing including a 2D brick-layer structure as found for TIPS-pentacene (Fig. 4) with very similar cell parameters (Supplementary data). Only a small difference of the mean interplane spacing was noticed (3.32 Å for TIPS-triphenodioxazine, 3.36 Å for TIPS-pentacene). Consequently, the cell volume was smaller (926 $Å^3$ vs 961 $Å^3$) and density was higher for the triphenodioxazine derivative (1.16 g/cm^3 vs 1.1 g/cm^3).

Secondly, the X-ray diffractograms recorded out on the OFET samples mainly showed sharp (00c) diffraction peaks at lower angles over an undulating baseline due to the polystyrene underlayer, corresponding to interplanar

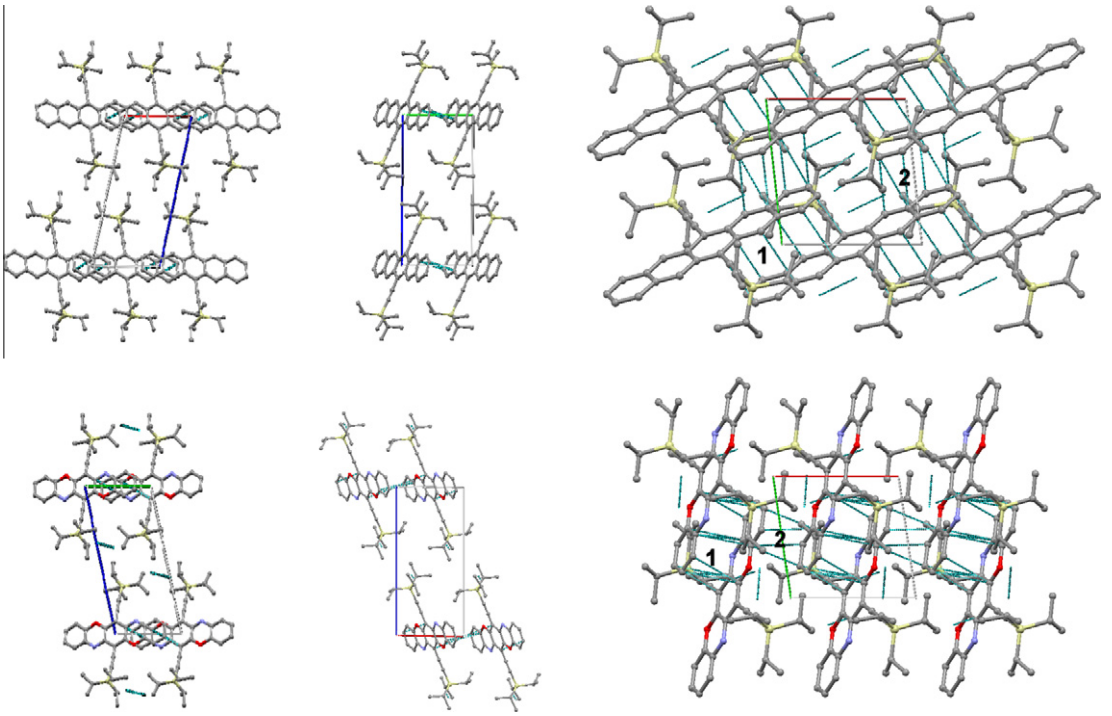

Fig. 4. TIPS-pentacene (top, redrawn from [25]) and TIPS-triphenodioxazine (bottom) crystal packings (projection onto ac, bc and ab plane from left to right; atom hydrogens are hidden).

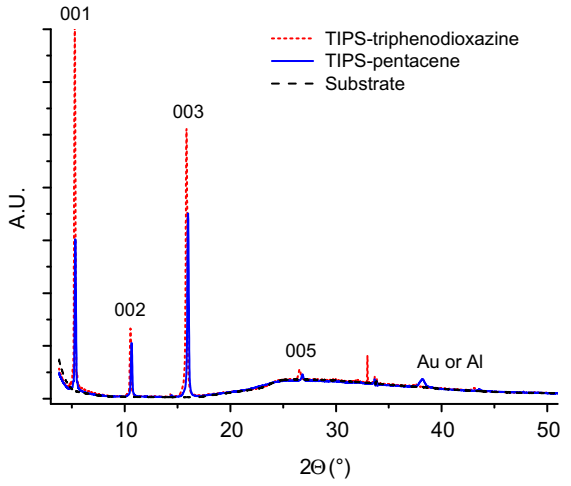

Fig. 5. XRD patterns of TIPS-pentacene (blue line), TIPS-triphenodioxazine (red dotted line) and polystyrene (black dashed line) (For interpretation of the references to color in this figure legend, the reader is referred to the web version of this article).

distances of 1.67 and 1.66 nm for TIPS-triphenodioxazine and TIPS-pentacene, respectively (Fig. 5). Moreover, the full width at half maximum of the first peak was 0.134° for both materials. As previously observed for TIPS compounds [25,36], the pattern showing only (00c) diffraction peaks along with the corresponding line-width indicates the formation of oriented polycrystalline films.

Finally, according to topographic AFM images recorded in the tapping mode, the thin films obtained by sublimation were polycrystalline and made of grains whose size was about 500 nm in both cases (Fig. 6). Moreover, few terraces were observed for TIPS-triphenodioxazine with a mean height of 1.6 nm (Fig. 7), which corresponds to the c lattice parameter found in the X-ray structure of TIPS-triphenodioxazine (Supplementary data) and the interplanar distance obtained by X-ray powder diffraction. As a result, the 2D π-stacking was oriented parallel to the substrate that constitutes a key requirement for high efficiency OFET architectures.

3.4. OFET properties

The semiconducting properties of TIPS-triphenodioxazine were examined in bottom-gate top contact OFET devices and compared to those of TIPS-pentacene under similar conditions. The substrate was composed of a 200 nm thermally grown SiO_2 layer on highly N-doped silicon layers. A layer of 150 nm of polystyrene (PS) was spin-coated over the silica layer after pre-treatment with hexamethyldisilazane (HMDS). After sublimation of 35 nm thick films of organic compounds on the substrate at ambient temperature, aluminum or gold top electrodes were evaporated through a shadow mask [37]. The optimization of device fabrication has encompassed the thickness of organic semiconductors, the substrate temperature during the depositions and the choice of the dielectric layer among the following materials: Self-Assembled Monolayer (SAM) of octatrichlorosilane (OTS) over 200 nm of SiO_2,

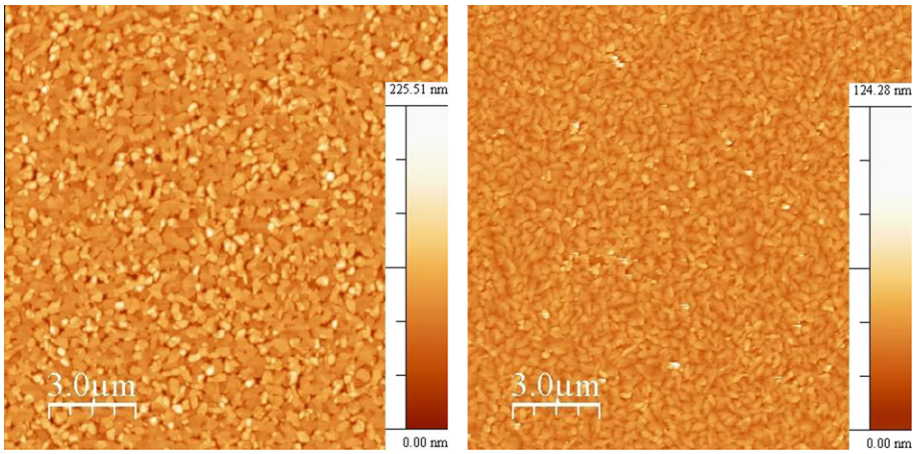

Fig. 6. AFM topographic images (15 × 15 µm^2) of TIPS-pentacene (left) and TIPS-triphenodioxazine (right).

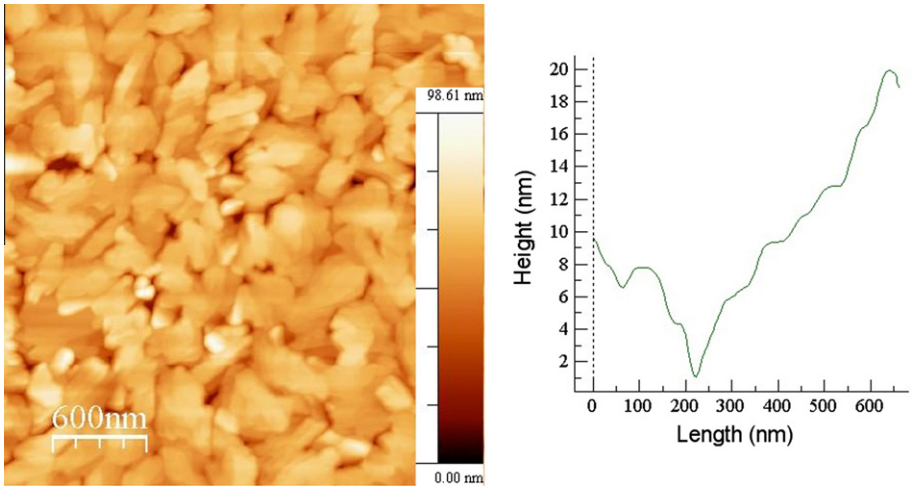

Fig. 7. AFM topographic images of TIPS-triphenodioxazine (3 × 3 µm^2) (left) and line profile (right).

Table 2
Properties of top-contact OFETs based on C_{60}, TIPS-pentacene and TIPS-triphenodioxazine.

Comp.	Elect.	μ_h (cm^2 V^{-1} s^{-1})	μ_e (cm^2 V^{-1} s^{-1})	I_{on}/I_{off}	V_{th} (V)
C_{60}	Al	–	0.8	10^6	26
TIPS-pentacene	Al	–	5×10^{-5}	10	5
	Gold	7×10^{-3}	–	10^5	−15
TIPS-triphenodioxazine	Al	–	4×10^{-3}	10^4	9
	Gold	–	–	–	–

25 nm of PS over OTS-treated SiO_2, and 150 nm of PS over HMDS-treated SiO_2. Additionally, reference OFETs have been elaborated with TIPS-pentacene following the procedure described by Sheraw et al. [24]. All measurements have been performed under inert atmosphere.

Reference n-type OFETs based on C_{60} as organic semiconductor showed a mobility of 0.8 cm^2 V^{-1} s^{-1}, which validates the fabrication process since the mobility obtained fall within the range of that reported for n-type OFETs involving C_{60} and aluminum electrodes [37]. Similarly, the reference TIPS-pentacene OFETs led to classical characteristics (average mobility of 0.49 cm^2 V^{-1} s^{-1}). The dielectric layers containing OTS led to unstable n-type OFETs, contrary to the layer of PS over HMDS-treated SiO_2. The capacitance per unit area, measured from substrates without semiconducting layer, is equal to 6.9 nF cm^{-2}, which is close to calculated value (7.8 nF cm^{-2} with $\varepsilon_r = 2.4$ for polystyrene). The results obtained for TIPS-pentacene and

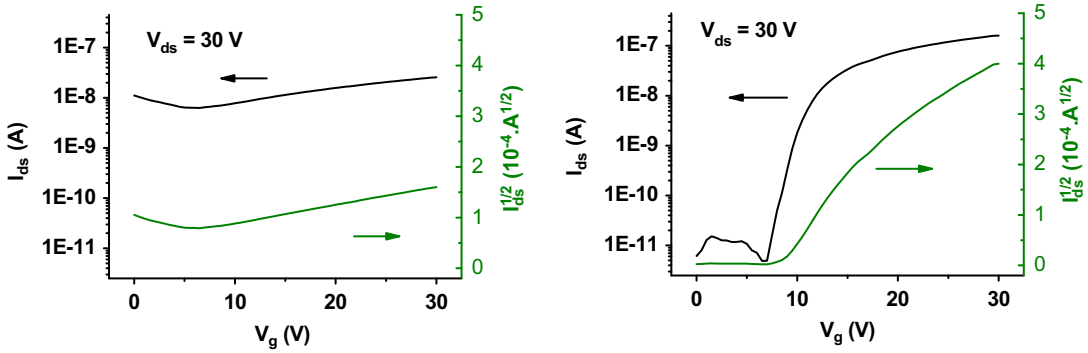

Fig. 8. Transfer curves for TIPS-pentacene (left) and TIPS-triphenodioxazine (right).

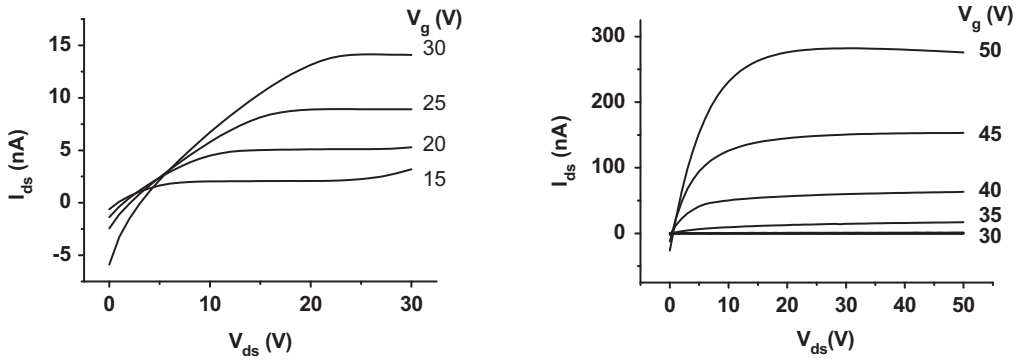

Fig. 9. Output curves for TIPS-pentacene (left) and TIPS-triphenodioxazine (right).

TIPS–triphenodioxazine are reported in Table 2. With gold electrodes, p-type charge transport was observed for TIPS-pentacene as previously reported [24], while no field effect conduction was detected with TIPS-triphenodioxazine. This behavior can be attributed to the higher potential barrier between the ionization potential of the semiconductor and the work function of gold for triphenodioxazine derivatives impeding charge injection through the metal/semiconductor interface [38].

Using aluminum electrodes, no p-type field effect was observed in both cases. As previously, the absence of field effect conduction under a negative gate bias potential can be related to the high potential barrier between the work function of aluminum and the ionization potential of the semiconductor materials that prevents hole injection. In contrast, n-type field-effect was detected for both materials (Figs. 8 and 9). Thus, TIPS-triphenodioxazine layers showed improved n-type OFET performances with an electron field-effect mobility and a I_{on}/I_{off} ratio of 4×10^{-3} cm^2 V^{-1} s^{-1} and 10^4, respectively. By comparison, TIPS-pentacene layers led to a decrease of the OFET characteristics from p-type to n-type architectures.

3.5. Theoretical modeling

To gain further insight into the enhancement of the n-type mobility with TIPS-triphenodioxazine compared to TIPS-pentacene semiconducting layers, we performed quantum chemical calculations of the main electronic parameters governing the charge transport efficiency (see Supporting Information). These calculations demonstrated that the differences in electron mobility performances between the two materials cannot be attributed neither to differences in the strength of intermolecular electronic couplings nor to differences in the reorganization energies. This suggests that the electron mobility of TIPS-pentacene and TIPS-triphenodioxazine is not intrinsic, although the X-ray diffractograms of the two materials are quite similar. As suggested by a recent theoretical study [39], one possible origin of the different n-type mobilities might be ascribed to differences in the intimate morphology of the dielectric layers interfacing with the insulating layer, which cannot be grasped by X-ray measurements. Indeed, electrostatic interactions with the substrate can induce an energetic disorder in the first organic dielectric layer, where the majority of charge carriers get accumulated in the OFETs, which in turn alters the charge transport performances. In our case, the larger μ_e value measured using TIPS-triphenodioxazine might thus be attributed to a smaller dispersion in the site energies in the interfacial organic layer.

4. Conclusions

An innovative synthetic pathway towards the triphenodioxazine core has been developed to provide soluble

organic n-type semi-conducting materials. As chemical structure of organic semiconductor in OFET, TIPS-triphenodioxazine led to electronic mobilities that outperformed by two orders of magnitude those of TIPS-pentacence measured under similar conditions. This significant enhancement of the n-type mobility cannot be explained neither by the electronic structures of the two isolated compounds, which have close electron affinities, nor to the differences in their supramolecular packing owing to their very similar thin film topography and X-ray diffraction patterns. Quantum chemical calculations of the electronic parameters driving the charge transport in the framework of the Marcus–Jortner theory, namely the transfer integrals and the reorganization energies, did not provide any further information. Nonetheless, the two molecules showed dissimilar spatial distribution of the frontier orbitals and the anion of TIPS-triphenodioxazine showed a higher stability regarding its chemical reactivity, which could be at the origin of the enhanced n-type performances of TIPS-triphenodioxazine-based OFET. As other hypothesis, electrostatic interactions between the substrate and the first organic layer, which are different in the two materials owing to the presence of local dipoles in the TIPS-triphenodioxazine core, might generate an energetic disorder affecting the charge transport performances. Despite these opened questions, the triphenodioxazine core appears as a promising candidate to design new organic n-type semiconducting materials. The synthesis of new dioxazine derivatives in that purpose is currently in progress.

Acknowledgements

The University of Bordeaux 1, the CNRS, and the GIS "Advanced Materials in Aquitaine" are acknowledged for financial support. Electrospray mass spectra and MALDI-MS spectra were performed by the CESAMO (Bordeaux, France). Elemental microanalyses were performed at the "Service Central d'Analyse du CNRS" (Vernaison, France). Calculations were carried out on mainframe computers of the "Mésocentre de Calcul Intensif Aquitain" (MCIA) of the University Bordeaux I, financed by the Conseil Régional d'Aquitaine and the French Ministry of Research and Technology.

Appendix A. Supplementary data

Supplementary data associated with this article can be found, in the online version, at http://dx.doi.org/10.1016/j.orgel.2012.04.010.

References

[1] H. Klauk, Organic Electronics: Materials, Manufacturing and Applications, first ed., Wiley-VCH, 2006.
[2] S.R. Forrest, Nature 428 (2004) 911.
[3] T. Sekitani, U. Zschieschang, H. Klauk, T. Someya, Nat. Mater. 9 (2010) 1015.
[4] B. Crone, A. Dodabalapur, Y. Lin, R. Filas, Z. Bao, A. LaDuca, R. Sarpeshkar, H. Katz, W. Li, Nature 403 (2000) 521.
[5] A. Dzwilewski, P. Matyba, L. Edman, J. Phys. Chem. B 114 (2010) 135.
[6] H. Klauk, U. Zschieschang, J. Pflaum, M. Halik, Nature 445 (2007) 745.
[7] L. Pouchain, O. Alévêque, Y. Nicolas, A. Oger, C.-H. Le Régent, M. Allain, P. Blanchard, J. Roncali, J. Org. Chem. 74 (2009) 1054.
[8] L.-Lay Chua, J. Zaumseil, J.-Fen Chang, E.C. Ou, Nature 434 (2005) 194.
[9] H. Klauk, Chem. Soc. Rev. 39 (2010) 2643.
[10] G. Llorente, M.-B. Dufourg-Madec, D.J. Crouch, R.G. Pritchard, S. Ogier, S.G. Yeates, Chem. Comm. 24 (2009) 3059.
[11] R.J. Chesterfield, J.C. McKeen, C.R. Newman, P.C. Ewbank, D.A. da Silva Filho, J.-L. Brédas, L.L. Miller, K.R. Mann, C.D. Frisbie, J. Phys. Chem. B 108 (2004) 19281.
[12] R. Schmidt, J.H. Oh, Y.-S. Sun, M. Deppisch, A.-M. Krause, K. Radacki, H. Braunschweig, M. Könemann, P. Erk, Z. Bao, F. Würthner, J. Am. Chem. Soc. 131 (2009) 6215.
[13] Z. Bao, A.J. Lovinger, J. Brown, J. Am. Chem. Soc. 120 (1998) 207.
[14] Md.M. Islam, S. Pola, Y.-T. Tao, Chem. Comm. 47 (2011) 6356.
[15] M.L. Tang, A.D. Reichardt, P. Wei, Z. Bao, J. Am. Chem. Soc. 131 (2009) 5264.
[16] Y.-C. Chang, M.-Y. Kuo, C.-P. Chen, H.-F. Lu, I. Chao, J. Phys. Chem. C 114 (2010) 11595.
[17] Z. Liang, Q. Tang, R. Mao, D. Liu, J. Xu, Q. Miao, Adv. Mater. 23 (2011) 5514.
[18] H. Bronstein, Z. Chen, R.S. Ashraf, W. Zhang, J. Du, J.R. Durrant, P.S. Tuladhar, K. Song, S.E. Watkins, Y. Geerts, M.M. Wienk, R.A.J. Janssen, T. Anthopoulos, H. Sirringhaus, M. Heeney, I. McCulloch, J. Am. Chem. Soc. 133 (2011) 3272.
[19] M. Mas-Torrent, C. Rovira, Chem. Soc. Rev. 37 (2008) 827.
[20] J. Zaumseil, H. Sirringhaus, Chem. Rev. 107 (2007) 1296.
[21] H. Yan, Z. Chen, Y. Zheng, C. Newman, J.R. Quinn, F. Dötz, M. Kastler, A. Facchetti, Nature 457 (2009) 679.
[22] Y. Wen, Y. Liu, Adv. Mater. 22 (2010) 1331.
[23] A.R. Murphy, J.M. Fréchet, Chem. Rev. 107 (2007) 1066.
[24] C.D. Sheraw, T.N. Jackson, D.L. Eaton, J.E. Anthony, Adv. Mater. 15 (2003) 2009.
[25] J.E. Anthony, J.S. Brooks, D.L. Eaton, S.R. Parkin, J. Am. Chem. Soc. 123 (2001) 9482.
[26] S.K. Park, T.N. Jackson, J.E. Anthony, D.A. Mourey, Appl. Phys. Lett. 91 (2007) 063514.
[27] Y.-Y. Liu, C.-L. Song, W.-J. Zeng, K.-G. Zhou, Z.-F. Shi, C.-B. Ma, F. Yang, H.-L. Zhang, X. Gong, J. Am. Chem. Soc. 132 (2010) 16349.
[28] Z. Liang, Q. Tang, J. Xu, Q. Miao, Adv. Mater. 23 (2011) 1535.
[29] C. -an Di, J. Li, G. Yu, Y. Xiao, Y. Guo, Y. Liu, X. Qian, D. Zhu, Org. Lett. 10 (2008) 3025.
[30] M. J. Frisch, G. W. Trucks, H. B. Schlegel, G. E. Scuseria, M. A. Robb, J. R. Cheeseman, G. Scalmani, V. Barone, B. Men-nucci, G. A. Petersson, H. Nakatsuji, M. Caricato, X. Li, H. P. Hratchian, A. F. Izmaylov, J. Bloino, G. Zheng, J. L. Sonnenberg, M. Hada, M. Ehara, K. Toyota, R. Fukuda, J. Hasegawa, M. Ishida, T. Nakajima, Y. Honda, O. Kitao, H. Nakai, T. Vreven, J. A. Montgomery Jr., J. E. Peralta, F. Ogliaro, M. Bearpark, J. J. Heyd, E. Brothers, K. N. Kudin, V. N. Staroverov, R. Kobayashi, J. Normand, K. Raghavachari, A. Rendell, J. C. Burant, S. S. Iyen-gar, J. Tomasi, M. Cossi, N. Rega, J. M. Millam, M. Klene, J. E. Knox, J. B. Cross, V. Bakken, C. Adamo, J. Jaramillo, R. Gomperts, R. E. Stratmann, O. Yazyev, A. J. Austin, R. Cammi, C. Pomelli, J. W. Ochterski, R. L. Martin, K. Morokuma, V. G. Zakrzewski, G. A. Voth, P. Salvador, J. J. Dannenberg, S. Dapprich, A. D. Daniels, Ö. Farkas, J. B. Foresman, J. V. Ortiz, J. Cio-slowski, D. J. Fox, Gaussian 09 Revision A.02 , Gaussian Inc., Wallingford CT, 2009.
[31] R.L. Mital, S.K. Jain, J. Chem. Soc. C (1971) 1875.
[32] S. Urgaonkar, J.G. Verkade, J. Org. Chem. 69 (2004) 5752.
[33] F.N. Ngassa, E.A. Lindsey, B.E. Haines, Tetrahedron 65 (2009) 4085.
[34] O.L. Griffith, A.G. Jones, J.E. Anthony, D.L. Lichtenberger, J. Phys. Chem. C 114 (2010) 13838.
[35] O.L. Griffith, J.E. Anthony, A.G. Jones, D.L. Lichtenberger, J. Am. Chem. Soc. 132 (2010) 580.
[36] S.C.B. Mannsfeld, M.L. Tang, Z. Bao, Adv. Mater. 23 (2010) 127.
[37] X.-H. Zhang, B. Domercq, B. Kippelen, Appl. Phys. Lett. 91 (2007) 092114.
[38] S.M. Sze, Semiconductor Devices, second ed., Wiley Interscience, 1981.
[39] N.G. Martinelli, M. Savini, L. Muccioli, Y. Olivier, F. Castet, C. Zannoni, D. Beljonne, J. Cornil, Adv. Funct. Mater. 19 (2009) 3254.